Parkinson's protein α-synuclein : membrane interactions and fibril structure

Kumar, P.

4 Characterization of Fibrils Obtained by Seeded Fibrillization of a Series of Spin-Labeled α-Synuclein Variants by Transmission Electron Microscopy

4.1 Introduction

The protein α-Synuclein (αS) is 140 amino-acids long and is present mainly in the human brain. The protein monomer is intrinsically disordered (1), which under certain conditions forms amyloid fibrils (2–9). Polymorphism of fibrils was described previously, for example, for Amyloid β (10), Immunoglobulin (Ig) light chains (11), ovalbumin (12), lysozyme (13), and also αS (14–17).

In an accompanying pulsed-EPR study (chapter 5), we sought to determine the inner intrinsic fold of αS in fibrils using αS with spin labels at different positions. For that, independent information about the fibril morphology was desired. The main question was whether the fibrils of all spin-label constructs have the same morphology. To do so, we prepared the fibrils of nine doubly spin-labeled variants (αS42/69, αS42/75, αS42/85, αS56/69, αS56/75, αS56/90, αS69/85, αS69/90, and αS75/85) and characterized the morphology by transmission electron microscopy (TEM). All the proteins were fibrillized as described in the Materials and methods section. We used the same fibrils for the successive EPR study in chapter 5.

In this study, we found that the morphology of the fibrils of all protein constructs grown under the conditions described in the present study is similar.

4.2 Materials and methods

4.2.1 Preparation of fibrillar αS

The expression, purification and MTSL-labelling of the protein αS has been described in chapter 5 (18–20).

4.2.1.1 Preparation of αS-fibril seeds

For seeds, we first prepared wild type (wt) αS fibrils following the protocol from Sidhu *et al*. (17). Briefly, the wt-αS protein solution (concentration = 100 µM, in 10 mM Tris- Cl buffer pH 7.4 containing 10 mM NaCl and 0.1 mM EDTA) was aliquoted into 15 Eppendorf tubes (Eppendorf LoProtein Bind 2 ml), 500 µl each. All tubes were incubated at a temperature of 37 ^{o}C shaking continuously at 500 rpm in a Thermo mixer (Eppendorf). The time evolution of αS fibrillization was monitored by the standard Thioflavin T (ThioT) fluorescence assay. For each tube, fibrillization was stopped when ThioT fluorescence intensity had reached a plateau. The fibrillization was completed in 6-7 days. The content of each Eppendorf tube was divided into two samples of 250 µl each, which were frozen quickly in liquid nitrogen and stored at - 20 ^{o}C. To start the seeded fibrillization experiment, one aliquot was thawed and sonicated in a bath sonicator (Branson 2510) for one minute to break the fibrils into seeds, which were then added to the samples to be fibrillized.

4.2.1.2 Seeded fibrillization of spin-labeled αS

We prepared the fibrils by mixing the monomeric αS (spin-labeled and wild type αS) with the wt-αS seeds. The total monomer concentration used for making fibrils was 100 µM. To this mixture 2 % monomer equivalent seeds were added.
Diamagnetic dilution was employed to diminish the effect of intermolecular interaction. We used 1:20 (SLαS:wt) diamagnetic dilution for all doubly labeled αS. A typical sample for doubly labeled αS consisted of 5 µM spin-labeled αS, 95 µM wt-αS and 2 µM αS-monomer equivalent seeds. The total volume for each sample was 3.0 ml, which was aliquoted into five Eppendorf tubes and put on the thermomixer. The seeded fibrillization was performed under the same conditions

as used for wt-αS fibrils (17). The time evolution of seeded fibrillization was monitored by the standard Thioflavin T (ThioT) fluorescence assay. Most of the mutants completed the aggregation, i.e., fluorescence intensity reached the plateau, in 24 hours except for αS69/90, which took 9 days to complete the aggregation. These samples, after harvesting, were used for the pulsed EPR experiments, described in chapter 5. A small amount of fibril solution from each sample was used to prepare TEM-grids to visualize the morphology.

4.2.1.3 Preparation of unseeded fibrils of αS69/90

The unseeded fibril of αS69/90 (referred to as ***αS69/90*** in the text) was prepared following the method described by Hashemi Shabestari *et al*. (21), described briefly. The total monomer concentration used for making fibrils was kept 100 µM. We used a diamagnetic dilution of 1:20 (SL αS:wt) similar to the seeded fibrillization case. The fibrillization mixture was prepared by mixing a 5 µM spin-labeled αS69/90 with 95 µM wt-αS protein in 10 mM Tris-Cl buffer, pH 7.4, containing 50 mM NaCl. The total volume of the mixture was 2.8 ml, which was aliquoted into four Eppendorf tubes (Eppendorf LoProtein Bind 2ml), 700 µl each. All tubes were incubated at a temperature of 37 ^{o}C with constant shaking at 1000 rpm in a Thermo mixer (Eppendorf). The time evolution of fibrillization was monitored by the ThioT assay. For each tube, fibrillization was stopped when the ThioT-fluorescence intensity reached a plateau. The fibrillization was completed in 6-7 days. A small amount of fibril solution was used for TEM and the remaining fibril solution was harvested as described above and double electron-electron resonance (DEER) experiment (see appendix B) was performed.

4.2.2 Transmission electron microscopy

Negative staining of αS fibril samples was done by placing a fresh carbon-coated grid (200 meshes) on top of a drop (10 µl) of the αS-fibril solution for 2 minutes. The grid was then washed 3 times on a drop of distilled water. Subsequently, the grids were placed directly on top of a small drop of 3.5 % uranyl acetate for 1.5 minutes and the excess uranyl acetate was blotted away by touching the grids to a filter paper at an angle of 45^{o}. Afterwards the grids were placed in a Petri dish with filter paper to let them dry. The grids were examined with a FEI Technai-12 G2 Spirit Biotwin transmission electron microscope (FEI, Eindhoven, Netherlands) and micrographs were taken with a Veleta side-mounted TEM camera using Radius acquisition software (both Olympus Soft Imaging Solutions, Münster, Germany). Images were measured using the image processing feature within the Radius software package.

4.3 Results

Figures 4.1 and 4.2 show the TEM images of αS fibrils prepared under seeded conditions. These Figures show that all fibrils used in this study have a similar appearance, which we describe in the following. Single fibrils have a width of 5.6 ± 1 nm (Figure 4.1a, bottom, black arrows) and are often found to twin with another fibril that runs parallel to generate a fibril with a width of 9-10 nm marked by black arrows (see Figure 4.1a & Figure 4.2g, middle, and Table 4.1). Many of these twinned fibrils are twisted. We further characterize twinned fibrils with the periodicity of the twist, measured between the points marked by white arrows in Figure 4.1c and 4.2f, middle. With the exception of αS56/75, αS75/85 and αS69/90, all fibrils show families of periodicities around 170 nm, 240 nm, and 290 nm. Fibrils of αS56/75 show periodicity around 53 nm, 103 nm, and 152 nm,

while fibrils of αS75/85 and αS69/90 show just one family of periodicity around 177 nm and 190 nm respectively.

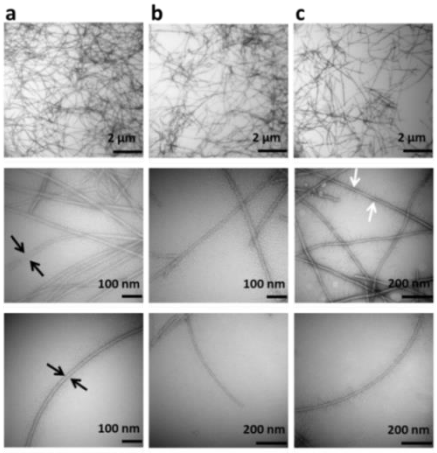

Figure 4.1. Morphological characterization of seeded fibrils of αS by TEM. a. αS42/69, b. αS42/75,c. αS42/85. Black arrows depict the width of a single fibril as shown for αS42/69 fibril. White arrows depict the points of cross-over of a twist in the fibril and the periodicity was measured between the points as shown for αS42/85 fibril.

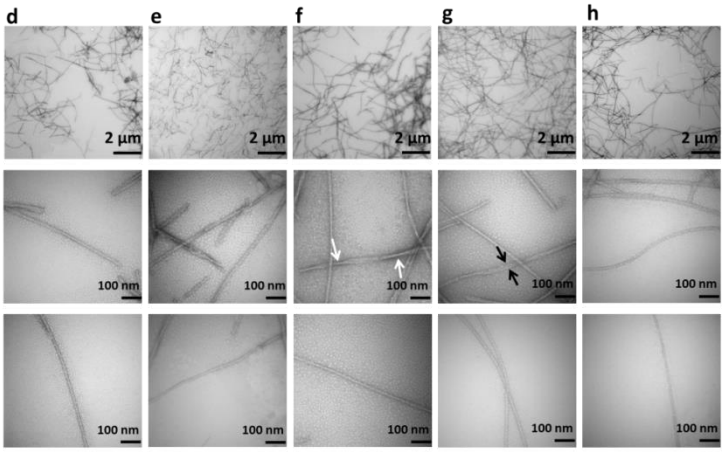

Figure 4.2. Morphological characterization of seeded fibrils of αS by TEM. d. αS56/69, e. αS56/75, f. αS56/90, g. αS69/85, and h. αS75/85. White arrows depict the points of cross-over of a twist in the fibril as shown for αS56/90. Black arrows depict the width of a twin fibril running together.

Table 4.1. Morphology parameters of Seeded fibrils of αS based on TEM

αS fibril sample	Single fibril width (nm) ± stdv (nm) [no of fibrils checked]	Twinned fibril width (nm) ± stdv (nm) [no of fibrils checked]	Periodicity (nm) ± stdv (nm) [no of fibrils checked]
αS42/69	5.5 ± 0.9 [17]	9.45 ± 1.0 [7]	182.5 ± 9.5 [10], 237.8 ± 7.9 [2], 285.7 ± 14.7 [2]
αS42/75	5.4 ± 1.0 [16]	10.6 ± 1.2 [5]	165.8 ± 8.6 [11], 235 [1]
αS42/85	6.0 ± 0.6 [36]	9.5 ± 1.6 [13]	164.3 ± 9.9 [11], 227.8 ± 15 [13], 293.4 ± 9.7 [4]
αS56/69	6.1 ± 1.1 [7]	9.0 ± 1.3 [9]	171.8 ± 7.7 [16], 242.2 ± 6.0 [4]
αS56/75	5.7 ± 1.0 [7]	10.6 ± 2.2 [4]	53 ± 6.0 [2], 103 ± 12.4 [2], 152 [1]
αS56/90	5.2 ± 1.1 [9]	9.2 ± 1.0 [6]	165 ± 6.0 [4], 206 ± 13.5 [12], 266.8 ± 11.4 [6]
αS69/85	6.3 ± 1.0 [9]	11.1 ± 2.3 [8]	181.2 ± 6.0 [2], 308.3 ± 6.0 [3]
αS69/90	5.7 ± 1.0[22]	8.7 ± 0.9 [4]	190.4 ± 6.0 [2]
αS75/85	5.0 ± 1.4 [5]	9.2 ± 0.1 [3]	177.4 ± 9.9 [5]

To illustrate the comparison of fibril morphology, we show the width and the periodicity of fibrils (given in Table 4.1) as a scatter plot in Figures 4a and b. Figure 4.3a shows the plot of the width of fibrils as a function of the type of fibrils (single and twinned fibril), and Figure 4.3b shows the plot of the periodicities of the fibrils. Figure 4.3a illustrates that the width of the fibrils are the same within the error margins of the measurement. Figure 4.3b shows that there are three distinct clusters of periodicities for most of the fibrils. With the exception of αS56/75, the

periodicity of the fibrils within the clusters agrees within experimental error. The fibrils of αS75/85 and αS69/90 show just one class of periodicity of 177 nm and 190 nm respectively, take into account the smallest number of observations compared to the other fibrils. For all fibril samples, the difference between the clusters of periodicities is around 50 nm.

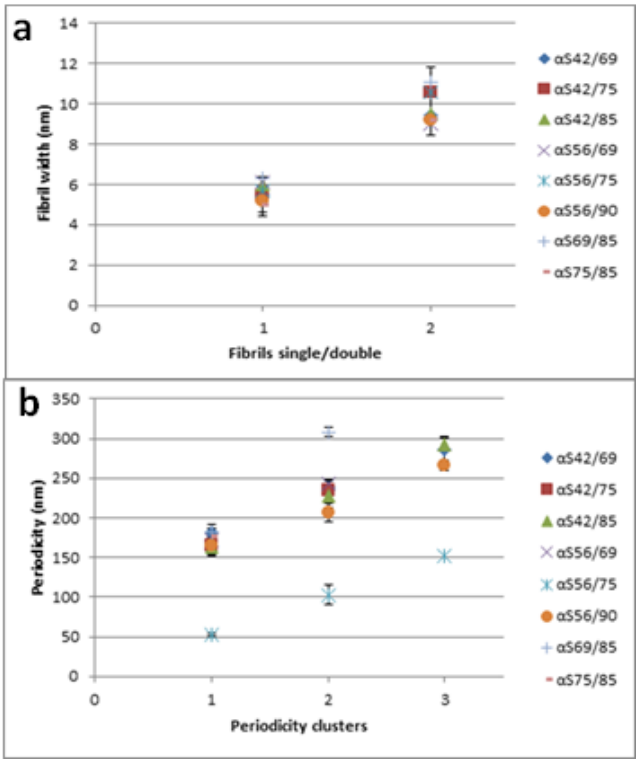

Figure 4.3. Scatter plots representing quantitative morphological features (listed in Table 4.1) of αS fibrils prepared under seeded condition (for details see Materials and methods): a. comparison of width of fibrils (given in Table 4.1); b. comparison of periodicities of fibrils (given in Table 4.1). Cluster 1: shortest periodicities; cluster 2: medium periodicities; cluster 3: longest periodicities.

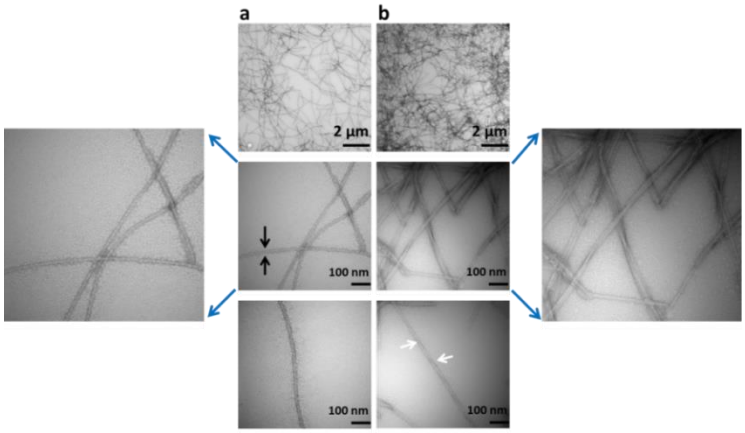

Figure 4.4. Morphological characterization of fibrils of αS by TEM. Comparision of morphology of the fibril prepared from the same αS69/90 protein a. under seeded conditions (for details, see Materials and methods); b. under the conditions described in Hashemi Shabestari *et al*. (21); Far left: middle panel of (a) scaled up (1.5x); Far right: middle panel of (b) scaled up (1.5x) for better view. Black arrows depict the width of the fibril, white arrows depict the points of cross-over.

Table 4.2. Comparision of fibril morphology of αS grown under seeded and unseeded conditions (21) based on TEM.

αS fibril sample	Single fibril width (nm) ± stdv (nm) [no of fibrils checked]	Twinned fibril width (nm) ± stdv (nm) [no of fibrils checked]	Periodicity (nm) ± stdv (nm) [no of fibrils checked]
αS69/90	5.7 ± 1.0[22]	8.7 ± 0.9 [4]	190.4 ± 6.0 [2]
αS69/90	5.6 ± 1.0 [9]	10.6 ± 1.2 [5]	116.6 ± 6.0 [4], 233 ± 8 [6], 278.7 ± 6.0 [3], 321.5 ± 9 [3], 352 [1]

Figure 4.4 shows the TEM images of fibrils prepared from the same αS69/90 protein, but under two different fibrillization conditions. Figure 4.4a shows the fibril morphology for the seeded-fibrillization conditions used in the present study (see Materials and methods), and Figure 4.4b for the fibrillization conditions

described in Hashemi Shabestari *et al*. (21,22). For clarity, we use the abbreviation ***αS69/90*** for the latter fibrils (21). Comparing the images in Figure 4.4a and b, in Figure 4.4b fibrils appear somewhat wider (far right, enlarged view) than fibrils in Figure 4.4a (far left, enlarged view). Single fibrils, in Figure 4.4a, have a width of 5.7 ± 1 nm (shown with black arrows and Table 4.2), similar to the width of the fibrils shown in Figure 4.4b (Table 4.2). Fibrils in seeded conditions show twinned fibrils of width 8.7 ± 0.9 and a periodicity of 190 ± 6 nm (as shown in Figure 4.4a and Table 4.2). On the other hand, twinned fibrils of ***αS69/90*** show twists with several different periodicity lengths (shown in Table 4.2 and Figure 4.4b; twists are indicated by white arrows). The separation between the periodicity lengths varies from 45 nm to 100 nm. The differences in morphology of fibrils, grown under seeded conditions and conditions described by Hashemi Shabestari *et al*. (21), are larger than those seen between fibrils grown from different spin-label constructs under the same conditions i.e., under seeded conditions.

4.4 Discussion

In this study, we have used a seeded fibrillization procedure employing the conditions described in A. Sidhu *et al*. (17) (see also Materials and methods) to prepare fibrils of homogeneous morphology. Fibrils of nine different αS spin-labelled variants were prepared and their morphology checked by negative stain Transmission Electron Microscopy (TEM). The overall appearance of the fibrils of all constructs is similar. The width of single fibrils and twinned fibrils in all constructs agree within the error margin of the measurement. From this, we conclude that the fibrils of all αS constructs have the same morphology. The origin of the differences in the periods of the twisted fibrils are not clear, but since different periods occur within one sample, it is likely that different periods do not affect the internal structure of the fibril, i.e., the fold of the protein within the

fibril. We also observe that fibrils grown under different conditions, i.e, αS69/90 and ***αS69/90***, have a difference in their TEM appearance (shown in Figure 4.4).

Fibrils isolated from the brain of patients of Parkinson's disease show a width of ~ 5 nm for a single untwisted αS-fibril (23), which is consistent with our finding in the present study. Vilar *et al*. (14) have reported αS-fibrils that were described as straight fibrils with a width of 5.5 ± 0.5 nm. They also reported that two such straight fibrils often run together with a width of 13 ± 1.0 nm. The single-fibril width in this case is in agreement with the fibril width for a single fibril found in our study. The difference between 10 nm and 13 nm for the width of twinned fibrils may be related to the arrangement of the two filaments. If the two filaments are associated sidewise, this will give a larger width, i.e., in the range of 11-13 nm, than if the two filaments are partly on top of each other, which could explain the lower value of the width in the range of 9-10 nm observed in the present study. Bousset *et al*. (15) have reported cylindrical fibrils with a width of 13 ± 2 nm, which may be caused by the lateral association of two to three filaments as discussed above.

Comparing our fibril morphology with that of Sidhu *et al*., (17) we note that a. the height measured by AFM is comparable to the width we observe, and b. the lengths of periods differ. In Sidhu *et al*., (17) at least 100 fibrils were measured and the periodicity given is averaged over the entire length of fibrils, selecting fibrils of minimally 1 μm long each. Such details could not be obtained in the present study, where we compare a large number of samples. Therefore, the periodicity information from the present study is less reliable than the one in Sidhu *et al*. (17). In addition, the differences in imaging methods, AFM and TEM, may lead to systematic variations in the parameters observed here and in Sidhu *et al*. (17).

In conclusion, we observed that the fibrils of different protein constructs grown under seeded conditions are similar in morphology. We also found that the difference in morphology for the fibrils, grown from the same protein under the seeded conditions and the conditions described in (21), i.e., unseeded conditions, is larger compared to those observed between fibrils grown under the seeded conditions. For direct comparison with previously published fibril morphologies (14,15,17,24,25), observation of a larger number of fibrils, higher resolution techniques like cryo-electron microscopy (cryo-EM) and mass-per-length-ratio measurements by scanning transmission electron microscopy (STEM) (26) would be needed. These were beyond the scope of the present investigation.

4.5 References

1. Weinreb PH, Zhen W, Poon AW, Conway KA, Lansbury PT. NACP, a protein implicated in Alzheimer's disease and learning, is natively unfolded. Biochemistry. 1996;35:13709–13715.

2. Spillantini MG, Schmidt ML, Lee VM, Trojanowski JQ, Jakes R, Goedert M. α-Synuclein in Lewy bodies. Nature. 1997;388:839–840.

3. Spillantini MG, Crowther RA, Jakes R, Hasegawa M, Goedert M. α-Synuclein in filamentous inclusions of Lewy bodies from Parkinson's disease and dementia with Lewy bodies. Proc Natl Acad Sci U S A. 1998;95:6469–6473.

4. Conway KA, Harper JD, Lansbury PT. Accelerated in vitro fibril formation by a mutant α-Synuclein linked to early-onset Parkinson disease. Nat Med. 1998;4:1318–1320.

5. El-Agnaf OM, Jakes R, Curran MD, Wallace A. Effects of the mutations Ala 30 to Pro and Ala 53 to Thr on the physical and morphological properties of α-Synuclein protein implicated in Parkinson's disease. FEBS Lett. 1998;440:67–70.

6. Hashimoto M, Hsu LJ, Sisk A, Xia Y, Takeda A, Sundsmo M, Masliah E. Human recombinant NACP/α-Synuclein is aggregated and fibrillated in vitro: Relevance for Lewy body disease. Brain Res. 1998;799:301–306.

7. Crowther RA, Jakes R, Spillantini MG, Goedert M. Synthetic filaments assembled from C-terminally truncated alpha-synuclein. FEBS Lett. 1998;436:309–12.

8. Hoyer W, Cherny D, Subramaniam V, Jovin TM. Impact of the acidic C-terminal region comprising amino acids 109−140 on α-Synuclein aggregation in vitro. Biochemistry. 2004;43:16233–16242.

9. Yagi H, Kusaka E, Hongo K, Mizobata T, Kawata Y. Amyloid fibril formation of α-Synuclein is accelerated by preformed amyloid seeds of other proteins: Implications for the mechanism of transmissible conformational diseases. J Biol Chem. 2005;280:38609–38616.

10. Goldsbury C, Frey P, Olivieri V, Aebi U, Müller SA. Multiple assembly pathways underlie amyloid-β fibril polymorphisms. J Mol Biol. 2005;352:282–298.

11. Ionescu-Zanetti C, Khurana R, Gillespie JR, Petrick JS, Trabachino LC, Minert LJ, Carter SA, Fink AL. Monitoring the assembly of Ig light-chain amyloid fibrils by atomic force microscopy. Proc Natl Acad Sci U S A. 1999;96:13175–13179.

12. Lara C, Gourdin-bertin S, Adamcik J, Bolisetty S, Mezzenga R. Self-assembly of ovalbumin into amyloid and non- amyloid fibrils. Biomacromolecules. 2012;13:4213-4221.

13. Adamcik J, Jordens S. General self-assembly mechanism converting hydrolyzed globular proteins into giant multistranded amyloid ribbons. Biomacromolecules. 2011;12:1868–1875.

14. Vilar M, Chou H, Lührs T, Maji SK, Riek-Loher D, Verel R, Manning G, Stahlberg H, Riek R. The fold of α-Synuclein fibrils. Proc Natl Acad Sci U S A. 2008;105:8637–8642.

15. Bousset L, Pieri L, Ruiz-Arlandis G, Gath J, Jensen PH, Habenstein B, Madiona K, Olieric V, Bockmann A, Meier BH, Melki R. Structural and functional characterization of two α-Synuclein strains. Nat Commun. 2013;4:1-13.

16. Gath J, Bousset L, Habenstein B, Melki R, Böckmann A, Meier BH. Unlike twins: An NMR comparison of two α-Synuclein polymorphs featuring different toxicity. PLoS One. 2014;9:1-11.

17. Sidhu A, Segers-Nolten I, Subramaniam V. Solution conditions define morphological homogeneity of α-Synuclein fibrils. Biochim Biophys Acta. 2014;1844:2127–2134.

18. van Raaij ME, Segers-Nolten IMJ, Subramaniam V. Quantitative morphological analysis reveals ultrastructural diversity of amyloid fibrils from α-Synuclein mutants. Biophys J. 2006;91:L96–L98.

19. Veldhuis G, Segers-Nolten I, Ferlemann E, Subramaniam V. Single-molecule FRET reveals structural heterogeneity of SDS-bound α-Synuclein. ChemBioChem.

2009;10:436–439.

20. Drescher M, Godschalk F, Veldhuis G, van Rooijen BD, Subramaniam V, Huber M. Spin-label EPR on α-Synuclein reveals differences in the membrane binding affinity of the two antiparallel helices. ChemBioChem. 2008;9:2411–2416.

21. Hashemi Shabestari M, Kumar P, Segers-Nolten IMJ, Claessens MMAE, van Rooijen BD, Subramaniam V, Huber M. Three long-range distance constraints and an approach towards a model for the α-Synuclein-fibril fold. Appl Magn Reson. 2015;46:369–388.

22. Hashemi Shabestari M. Spin-label EPR on disordered and amyloid proteins. Thesis, Leiden University Repository. 2013.

23. Crowther RA, Daniel SE, Goedert M. Characterisation of isolated α-Synuclein filaments from substantia nigra of Parkinson's disease brain. Neurosci Lett. 2000;292:128–130.

24. Heise H, Hoyer W, Becker S, Andronesi OC, Riedel D, Baldus M. Molecular-level secondary structure, polymorphism, and dynamics of full-length α-Synuclein fibrils studied by solid-state NMR. Proc Natl Acad Sci U S A. 2005;102:15871-15876.

25. Gath J, Habenstein B, Bousset L, Melki R, Meier BH, Böckmann A. Solid-state NMR sequential assignments of α-Synuclein. Biomol NMR Assign. 2012;6:51–55.

26. Tuttle MD, Comellas G, Nieuwkoop AJ, Covell DJ, Berthold DA, Kloepper KD, courtney JM, Kim JK, Barclay AM, Kendall A, Wan W, Stubbs G, Schwieters CD, Lee VM, Goerge JM, Rienstra CM. Solid-state NMR structure of a pathogenic fibril of full-length human α-Synuclein. Nat Struct Mol Biol. 2016;23:409–415.

Appendix B to chapter 4

To check whether the difference in fibrillization conditions for αS69/90 and ***αS69/90*** affects not only the morphology (see above), but also the internal structure, i.e., the fold of the protein inside fibrils, we performed DEER measurements on fibrils of αS69/90 and ***αS69/90***. Figure B1 shows the comparison of the DEER traces of αS69/90 and ***αS69/90***. The two traces look different. The modulation depth of ***αS69/90*** is larger than of αS69/90 (see Table 5.2 in chapter 5).The modulation depth of αS69/90 is small, therefore, the distance distribution of this sample is not meaningful, because only a small fraction of the spin population contributes to it. As both fibrillizations were made with the same protein batch, the difference in modulation depth shows that for αS69/90, less spin-pairs are in the sensitive distance range of DEER (2 nm – 5 nm), which we interpret as a difference in the internal αS-fold between the two types of fibrils, αS69/90 and ***αS69/90***.

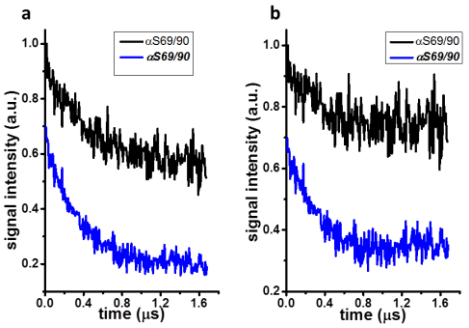

Figure B1. Comparision of DEER time traces of αS 69/90 fibril samples prepared under different fibrillization conditions: a. DEER time traces of αS69/90 (black lines) and ***αS69/90*** (blue lines) before background corrections, b. DEER time traces of both fibril samples after background correction (black line: αS 69/90, blue lines: ***αS 69/90***) (for details see text). Both the DEER traces are normalized to one by dividing the traces by the maximum of their intensity. DEER traces are shifted vertically with respect to each other for better visibility.